Phytochemistry Letters 55 (2023) 137–141

Contents lists available at ScienceDirect

Phytochemistry Letters

journal homepage: www.elsevier.com/locate/phytol

Three new isoquinoline alkaloids from the cigar tobacco-derived endophytic fungus *Aspergillus felis*

Yue-Yu Ma [a], Gui Pu [a], Xue-Ju Cha [a], Rui-Feng Xiong [a], Guang-Hai Zhang [b], Heng Yao [b], Mei-Fen Bao [c], Guang-Hui Kong [b], Yin-Ke Li [a], Qiu-Fen Hu [a,*], Yu-Ping Wu [b,*]

[a] Key Laboratory of Natural Products Synthetic Biology of Ethnic Medicinal Endophytes, Yunnan Minzu University, Kunming 650500, PR China
[b] Yunnan Academy of Tobacco Agricultural Sciences, Kunming 650021, PR China
[c] Kunming Institute of Botany, Chinese Academy of Sciences, Kunming 650201, PR China

ARTICLE INFO

Keywords:
Isoquinolines
Alkaloids
Aspergillus felis
Anti-tobacco mosaic virus (anti-TMV) activity

ABSTRACT

The isoquinoline alkaloids have attracted widespread attention from chemists and biologists due to their complex structures and prominent bioactivities. With the aims of screening for antiviral compounds produced by fungi, in this study, three new (**1**-**3**), together with four known (**4–7**) isoquinolines were isolated from the cigar tobacco-derived endophytic fungus *Aspergillus felis*. Their structures were determined by means of HRESIMS and NMR spectroscopic studies. Interestingly, an anti-TMV test revealed that compounds **2** and **4** showed high activity with inhibition rates of 43.2% and 38.4%, respectively. These rates are higher than those of the positive control ningnanmycin (33.2%). The isolation of the above isoquinolines may provide materials for the study of more potent anti-TMV inhibitors and contribute to an improved utilization of cigar tobacco-derived endophytic fungi.

1. Introduction

Endophytic fungi are prolific producers of various secondary metabolites, and many scientists have an interest in studying endophytic fungi as potential producers of novel and biological active compounds (Toghueo et al., 2020; Zheng et al., 2021). Among the numerous existing endophytic fungi, *Aspergillus* species constitute one of the most prolific sources of natural products with diverse chemical classes and interesting biological activities (Hagag et al., 2022; El-Hawary et al., 2020). In our previous work, bioactive metabolites such as alkaloids (Yang al, 2022b; Dai et al., 2023), diterpenoids (Wang et al., 2019), butyrolactones (Zhou et al., 2015a; Zhou et al., 2015b), isocoumarins (Zhou et al., 2016; Yang et al., 2022a), anthraquinones (Dai et al., 2022), and have been isolated from this fungal genus. As characteristic chemical components of *Aspergillus*, alkaloids are important molecules, not only for chemical reasons, but also for their diverse biological functions (Debnath et al., 2018; Moradi et al., 2018). The isoquinolines are a large group of alkaloids, which show diverse pharmacological activities (Yadav and Shah, 2021; Prabal and Gopinatha, 2010), and some isoquinolines have been isolated from *Aspergillus* strains (Li et al., 2020a; Chi et al., 2021; Liu et al., 2022).

Cigar tobacco is an important economic crop, which is widely planted in Yunnan province, and the high altitude and extensive sunlight results in Yunnan cigar tobacco having a unique flavor and aroma (Sun et al., 2020). In addition, the unparalleled special geographical environment of Yunnan has also supplied a unique microbial population in the fermentation process of cigar tobacco (Li et al., 2020b; Zheng et al., 2022). As a matter of course, this distinctive microbial population and rich microbial species in the fermentation process of cigar tobacco, provides a new source for the discovery of bioactive metabolites.

As a part of our continuing search for bioactive compounds from tobacco-derived endophytic fungi, a chemical study on the culture broth of an *Aspergillus felis* from cigar tobacco was carried out. As a result, three new (**1–3**) and four known isoquinoline alkaloids (**4-7**), were isolated from the EtOAc extract of its fermentation. This paper deals with the isolation, structural elucidation, and the anti-TMV activity of these compounds.

2. Results and discussion

The whole culture broth of *A. felis* was extracted with EtOAc. The extract was partitioned between EtOAc and 3% aqueous tartaric acid. The aqueous layer was adjusted to pH 9.5 with saturated Na_2CO_3 aq. and again extracted with EtOAc. The EtOAc-soluble alkaloidal material was

* Corresponding authors.
E-mail addresses: huqf_tg@163.com (Q.-F. Hu), jszxtg2015@163.com (Y.-P. Wu).

https://doi.org/10.1016/j.phytol.2023.05.006
Received 10 January 2023; Received in revised form 11 May 2023; Accepted 12 May 2023
Available online 16 May 2023

subjected repeatedly to column chromatography on silica gel, MCI, RP-18 and preparative-HPLC to afford compounds **1**-**7**, including three new isoquinolines, 6-acetyl-8-methoxy-3-methyl-isoquinoline (**1**), 6-acetyl-8-methoxy-3-hydroxymethyl- isoquinoline (**2**), and 6-(3-hydroxypropyl)− 8-methoxy-3-methyl-isoquinoline (**3**), along with four known natural products (**4**-**7**). Their structures are shown in Fig. 1 and the NMR data of **1**-**3** are listed in Table 1. The known compounds, 5,10-dihydropyrrolo[1,2-*b*] isoquinoline-6,7-diol (**4**) (Nord et al., 2019), TMC-120A (**5**) (Kohno et al., 1999), TMC-120 C (**6**) (Kohno et al., 1999), and puniceusine G (**7**) (Liu et al., 2022), were identified by comparison of their spectroscopic data with literature.

Compound **1** was obtained as an orange gum. Its molecular formula $C_{13}H_{13}NO_2$ was deduced from the HRESIMS which showed a pseudo-molecular $[M+Na]^+$ ion at *m/z* 238.0851, with 8 degrees of unsaturation. Its infrared spectrum exhibited bands due to carbonyl (-C═O at 1685 cm^{-1}) and aromatic rings (-C═C- at 1612, 1460 and 1375 cm^{-1}), and the UV spectrum showed absorption maxima at 238 and 312 nm, also suggesting the presence of an aromatic ring in the molecule.

The ^1H, ^{13}C, and DEPT NMR data of **1** displayed resonances for 13 carbons and 13 hydrogen atoms, which were ascribed to a 1,2,3,5-tetra-substituted benzene ring (C-6, C-8-C-10, H-5, H-7), an aromatic methine (C-4, H-4), an *N*-bearing aromatic methine (C-1, H-1), an *N*-bearing aromatic quaternary carbon (C-3), a methyl group (C-1′, H_3-1′), an acetyl group (C-2′, C-3′, H_3-3′), and a methoxy group (δ_C 55.9, δ_H 3.84 s). By comparing with published literatures, the ^1H and ^{13}C NMR data for compound **1** were highly similar to these of known compounds, 3-methyl-isoquinoline-6-carboxylic acid at C-1∼C-10 and C-1′ (Quang et al., 2010) or TMC-120 at C-1∼C-4, and C-1′ (Kohno et al., 1999); and this leaded us to speculate that **1** should be a 3-methyl-isoquinoline. By further analysis of the above NMR data, two aromatic methines (C-1, C-4, H-1, and H-4), a quaternary carbon (C-3), a methyl (C-1′, H_3-1′), and a nitrogen atom (N-2) could be incorporated with the benzene to form an 3-methyl-isoquinoline to support the existence of two *N*-bearing aromatic carbons (C-1 and C-4) and 8 degrees of unsaturation. In addition, the existence of isoquinoline moiety can further be confirmed by the HMBC correlations from H-1 to C-3/C-8/C-9/C-10, from H-4 to C-5/C-10, from H-5 to C-4/C-9/C-10. The HMBC correlations from H_3-1′ to C-3/C-4, from H4 to C-1′ also supported that the methyl located at C-3.

Since the skeleton (3-methyl-isoquinoline) of the compound was determined unambiguously, the remaining signals (acetyl and methoxyl) could be considered as a substituents, and the existence of acetyl was supported by the comparison of typical acetyl signals (δ_C 26.4 (-CH_3) and 196.9 (-C═O, δ_H 2.53 (-CH_3)) with known compound (Yin et al., 2022), and the HMBC correlation from H_2-3′ to C-2′ in NMR spectra. Moreover, the acetyl group linked to C-6 was established by HMBC correlations from H-5 to C-2′, and from H_3-3′ to C-6, and the position of the methoxy group at C-8 was supported by an HMBC correlation from the methoxy protons (δ_H 3.84 s) to C-8. Additional, the typical proton signals on the benzene ring (8.04, d (2.2) and 7.55, d (2.2)) was also consistent with the 6,8-substitution on the isoquinoline. Hence, the structure of **1** was fully assigned, and given the systematic name 6-acetyl-8-methoxy-3-methyl-isoquinoline, which is a new natural product and described here for the first time.

Table 1
^1H and ^{13}C NMR data of compounds **1**–**3** ($CDCl_3$, δ in ppm).

No.	**1**		**2**		**3**	
	δ_C	δ_H (*J* in Hz)	δ_C	δ_H (*J* in Hz)	δ_C	δ_H (*J* in Hz)
1	145.8 (CH)	9.46, s	145.3 (CH)	9.53, s	145.7 (CH)	9.35 s
2-NH						
3	152.4 (C)		153.3 (C)		151.6 (C)	
4	120.6 (CH)	7.83, s	120.2 (CH)	7.90, s	118.6 (CH)	7.66, s
5	119.6 (CH)	8.04, d (2.2)	119.5 (CH)	8.11, d (2.2)	117.0 (CH)	7.02, d (2.2)
6	140.9 (C)		140.7 (C)		142.4 (C)	
7	102.5 (CH)	7.55, d (2.2)	102.7 (CH)	7.56, d (2.2)	105.6 (CH)	7.39, d (2.2)
8	154.4 (C)		154.3 (C)		153.7 (C)	
9	118.5 (C)		118.6 (C)		117.7 (C)	
10	139.6 (C)		139.3 (C)		137.8 (C)	
1′	23.7 (CH_3)	2.67, s	65.3 (CH_2)	5.15, s	23.7 (CH_3)	2.52, s
2′	196.9 (-C═O)		196.7 (-C═O)		32.8 (CH_2)	2.75, t (7.2)
3′	26.4 (CH_3)	2.53, s	26.4 (CH_3)	2.55, s	35.4 (CH_2)	1.92, m
4′					63.4 (CH_2)	3.66, t (6.2)
-OMe	55.9 (CH_3)	3.84, s	56.0 (CH_3)	3.83, s	56.0 (CH_3)	3.84, s

6-Acetyl-8-methoxy-3-hydroxymethyl-isoquinoline (**2**) was also obtained as an orange gum. Its molecular formula ($C_{13}H_{13}NO_3$) was determined by the presence of a quasi-molecular ion at *m/z* 318.1114 $[M+Na]^+$ observed in its HRESIMS (calcd. for $C_{13}H_{13}NNaO_3$, 318.1106). The ^1H and ^{13}C NMR spectral data of **2** (with the exception of the resonance for C-1) were highly similar to those of **1**. The obvious chemical shift differences resulted from the disappearance of methyl resonance and the appearance of an hydroxymethyl group (C-1′, H_2-1′). These changes indicated that **2** should by a 3-hydroxymethyl analogues

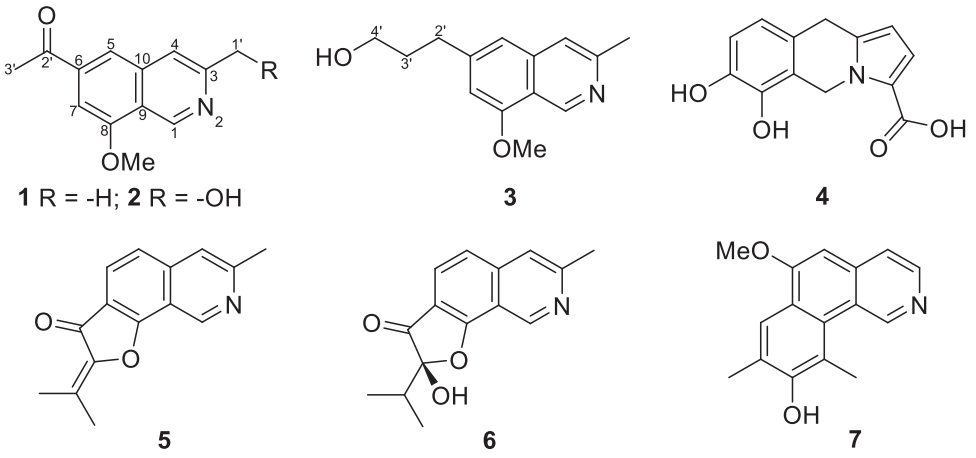

Fig. 1. The structures of isoquinolines from the fungus *A. felis*.

of **1**, and the hydroxymethyl group located at C-3 was supported by the HMBC correlations from H_2-1′ to C-3/C-4, from H-4 to C-1′. In addition, the acetyl group located at C-6 and the methoxy group located at C-8 were also confirmed by further analysis of it HMBC correlations. Therefore the structure of **2** was determined as shown in Fig. 1. Fig. 2.

The molecular formula of compound **3** was determined as $C_{14}H_{17}NO_2$ according to an ion peak at *m/z* 286.1050 ($[M+Na]^+$) in the HRESIMS. The UV and IR spectra and NMR signal patterns of **3** were also highly similar to those of **1** in C-1-C-10 and C-1′. The obvious difference was due to the replacement an acetyl group in **1** to a 3-hydroxypropyl group. (-$CH_2CH_2CH_2$-OH, C-2′-C-4′, H_2-2′-H_2-4′) in **3**. The existence of 3-hydroxypropyl group was supported by the comparison of typical NMR signals (δ_C 32.8 (-CH_2-), 35.4 (-CH_2-), and 63.4 (-CH_2OH); δ_H 2.75 t (7.2), 1.92 m, and 3.66 t (6.2)) with known compound (Yang et al., 2022a), and the HMBC correlations from H_2-2′ to C-3′/C-4′, from H_2-4′ to C-2′/C-3′, and from H_2-3′ to C-2′/C-4′. Moreover, the HMBC correlations from H_2-2′ to C-5/C-6/C-7, and from H_2-3′ to C-6 also supported that the 3-hydroxypropyl group attached at C-6 of the isoquinoline core. In addition, the positions of the methyl and methoxy groups were determined by further analysis of their HMBC correlations. The structure of 6-(3-hydroxypropyl)− 8-methoxy- isoquinoline (**3**) was therefore defined.

Since some isoquinolines have been shown to exhibit antiviral activity (Hu et al., 2020; Luo et al., 2020; Qing et al., 2017), compounds **1-7** were tested for their anti-TMV activities. This was achieved by the half-leaf method using ningnanmycin ($C_{16}H_{25}N_7O_8$, CAS#: 156410–09–2), a commercial product for plant disease in China, with an inhibition rate of 33.2% as the positive control (Yang et al., 2022b; Yang et al., 2022c; Hu et al., 2022). The results (Table 2) revealed that compounds **2** and **4** showed moderate anti-TMV activities with inhibition rates of 43.2% and 38.4%, respectively. These were higher than that of the positive control, and compounds **1, 3** and **5–7** also showed anti-TMV activities with inhibition rates in the range of 22.6% − 32.8%, respectively.

Table 2
Anti-TMV activities of compounds **1-7** on *N. glutinosa* Leaf.

No.	% Inhibition at 20 μM	IC_{50} (μM)
1	30.6 ± 2.5	41.2
2	43.2 ± 2.6	23.3
3	32.8 ± 2.4	35.5
4	38.4 ± 2.2	26.5
5	22.6 ± 2.0	49.4
6	26.8 ± 2.3	44.5
7	24.5 ± 2.5	47.8
Ningnanmycin	33.2 ± 2.4	34.2

[1]All results are expressed as mean ± SD; n = 3

3. Materials and methods

3.1. General experimental procedures

UV spectra were obtained using a Shimadzu UV-2401A spectrophotometer. A Tenor 27 spectrophotometer was used for scanning IR spectroscopy with KBr pellets. 1D- and ^{2}D NMR spectra were recorded on a DRX-500 spectrometer with TMS as internal standard and the chemical shifts (δ) were expressed in ppm. HRESIMS were performed on an API QSTAR time-of-flight spectrometer and a VG Autospec-3000 spectrometer. Preparative-HPLC was performed on a Shimadzu LC-8A preparative liquid chromatograph equipped with a UV detector and a Venusil MP C_{18} (20 mm × 25 cm, 5 μm) column. The detection wavelengths were set to 400, 275 and 250 nm. Column chromatography was performed with Si gel (200–300 mesh, Qing-dao Marine Chemical, Inc., Qingdao, China). The fractions were monitored by TLC, and spots were visualized by heating Si gel plates sprayed with 5% H_2SO_4 in EtOH.

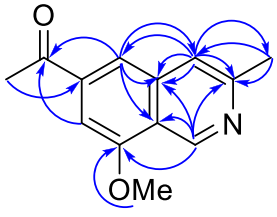

Fig. 2. Key HMBC correlations of **1**.

3.2. Fungal material

A culture of *Aspergillus felis* 0260 was isolated from the leaves of cigar tobacco, collected from the fermentation plant of Yuanjiang County, Yuxi Prefecture, Yunnan Province in 2020. The strain was identified by one of the authors (Dr. Yin-Ke Li) based on BLAST analysis of its ribosomal internal transcribed spacer (ITS) sequence data (GenBank accession no. OQ152598) contained in the NCBI database. This fungal strain was deposited in the Key Laboratory of Natural Products Synthetic Biology of Ethnic Medicinal Endophytes, Yunnan Minzu University. It was cultivated at room temperature for 7 days on potato dextrose agar at 28 °C. Agar plugs were inoculated into 250 mL Erlenmeyer flasks each containing 100 mL potato dextrose broth and cultured at 28 °C on a rotary shaker at 180 rpm for five days. Large scale fermentation was carried out in 100 Fernbach flasks (1.0 L) each containing 500 g of rice and 300 mL of nutrient solution (glucose 5%; peptone 0.15%; yeast 0.5%; KH_2PO_4 0.05%; urea 0.1%; $MgSO_4$ 0.05% in 1.0 L of deionized water; pH 6.5 before autoclaving). Each flask was inoculated with 5.0 mL of cultured broth and incubated at 27 °C for 20 days.

3.3. Extraction and isolation

The whole culture broth of *A. felis* was extracted four times with EtOH (4 ×25 L) at room temperature and filtered. The extract was partitioned between EtOAc and 3% aqueous tartaric acid. The aqueous layer was adjusted to pH 9.5 with saturated Na_2CO_3 aq. and extracted with EtOAc. The crude extract (69.24 g) was applied to silica gel column chromatography, eluting with a $CHCl_3$-MeOH gradient system (9:1, 8:2, 7:3, 6:4, 5:5). Five fractions were obtained from the silica gel column and individually decolorized on MCI gel to yield fractions A–E. Further separation of fraction A (9:1, 9.26 g) by silica gel column chromatography, eluting with $CHCl_3$-$(Me)_2CO$ (9:1, 8:2, 7:3, 6:4, 1:1), yielded sub-fractions A1–A5. Sub-fraction A2 (8:2, 1.92 g) was subjected to RP-18 column chromatography (MeOH/H_2O 40:60–80:20 gradient) and HPLC to give **5** (14.4 mg) and **7** (16.2 mg). Sub-fraction A2 (8:2, 1.15 g) was subjected to RP-18 column chromatography (MeOH/H_2O 30:70–70:30 gradient) and HPLC to give **1** (13.9 mg), **3** (15.4 mg) and **6** (14.2 mg). Sub-fraction A3 (7:3, 1.24 g) was subjected to RP-18 column chromatography (MeOH/H_2O 30:70–60:40 gradient) and HPLC to give **2** (12.9 mg). The further separation of fraction C (7:3, 9.64 g) by silica gel column chromatography, eluting with $CHCl_3$-$(Me)_2CO$ (7:3, 6:4, 1:1, 4:6, 3:7), yielded sub-fractions C1–C5. Sub-fraction C-2 (6:4, 1.22 g) was subjected to RP-18 column chromatography (MeOH/H_2O 20:80–60:40 gradient) and HPLC to give **4** (12.9 mg).

3.3.1. 6-Acetyl-8-methoxy-3-methyl-isoquinoline (1)

Orange gum; UV (MeOH) λ_{max} (log ε) 215 (4.02), 238 (3.86), 354 (3.64); IR ν_{max} 3082, 1685, 1612, 1460, 1375, 1354, 1278, 1134, 1039, 826 cm^{-1}; ^{1}H and ^{13}C NMR data (500 and 125 MHz), see Table 1; positive ESIMS *m/z* 238 $[M+Na]^+$, positive HRESIMS *m/z* 238.0851 (calcd. for $C_{13}H_{13}NNaO_2$, 238.0844).

3.3.2. 6-acetyl-8-methoxy-3-hydroxymethyl-isoquinoline (2)

Orange gum; UV (MeOH) λ_{max} (log ε) 215 (4.08), 242 (3.72), 358 (3.60); IR ν_{max} 3402, 3070, 1682, 1614, 1456, 1376, 1349, 1274, 1136, 1052, 819 cm^{-1}; ^{1}H and ^{13}C NMR data (500 and 125 MHz), see Table 1; positive ESIMS *m/z* 254 $[M+Na]^+$, positive HRESIMS *m/z* 254.0799 (calcd for $C_{13}H_{13}NNaO_3$, 254.0793).

3.3.3. 6-(3-hydroxypropyl)− 8-methoxy-3-methyl-isoquinoline (3)

Orange gum; UV (MeOH) λ_{max} (log ε) 215 (4.06), 232 (3.83), 346 (3.68); IR ν_{max} 3405, 3074, 1615, 1468, 1380, 1359, 1262, 1146, 1048, 842 cm^{-1}; ^{1}H and ^{13}C NMR data (500 and 125 MHz), see Table 1; positive ESIMS *m/z* 254 $[M+Na]^+$, positive HRESIMS *m/z* 254.1166 (calcd for $C_{14}H_{17}NNaO_2$, 254.1157).

3.4. Anti-TMV assay

The anti-TMV activities were tested using the half-leaf method (Yang et al., 2022b; Yang et al., 2022c; Hu et al., 2022), and ningnanmycin (a commercial product for plant disease in China), was used as the positive control. The virus was inhibited by mixing with a solution of test compounds. After 30 min, the mixture was inoculated on the left side of the leaves of *Nicotiana glutinosa*, whereas the right side of the leaves was inoculated with the mixture of DMSO solution and the virus as control. The local lesion numbers were recorded 3–4 days after inoculation. Three repetitions were conducted for each compound. The inhibition rates were calculated according to the formula:

$$\text{inhibition rate } (\%) = [\,(C\text{-}T) / C\,] \times 100\%$$

where C is the average number of local lesions of the control and T is the average number of local lesions of the treatment. Ningnanmycin, a commercial virucide for plant disease in China, was used as the positive control.

Declaration of Competing Interest

No potential conflict of interest was reported by the authors.

Data Availability

Data will be made available on request.

Acknowledgements

This project was supported financially by the Foundation of China Tobacco Monopoly Bureau Grants and Yunnan Provincial Tobacco Monopoly Bureau Grants (No. 2022530000241002, 110202103018), the National Natural Science Foundation of China (No. 32260111), and the Foundation of Yunnan Innovative Research Team (2019HC020).

Appendix A. Supporting information

Supplementary data associated with this article can be found in the online version at doi:10.1016/j.phytol.2023.05.006.

References

Chi, L.P., Li, X.M., Wan, Y.P., Li, Y.H.X., Li, Wang, B.G., 2021. Two new phenol derivatives from the cold seep-derived fungus *Aspergillus insuetus* SD-512. Chem. Biodivers. 18, e2100512.

Dai, J.M., Zhu, L.C., Xiao, D., Xie, J., Wang, X., Shi, J.Q., Yin, G.Y., Yang, Y.K., Yang, G. Y., Hu, Q.F., Wang, K., 2022. Two new anthraquinones from the cigar tobacco-derived fungus *Aspergillus versicolor* and their bioactivities. Chem. Nat. Compd. 58, 1001–1005.

Dai, J.M., Mi, Q., Li, Li, X.M., Du, G., Yang, G.Y., Zhang, J.D., Wang, J., Li, Y.K., Yang, H. Y., Dong, M., Li, Z.J., Hu, Q.F., 2023. The anti-TMV potency of the tobacco-derived fungus *Aspergillus versicolor* and its active alkaloids, as anti-TMV activity inhibitors. Phytochemistry 205, 113485.

Debnath, B., Singh, W.S., Das, M., Goswami, S., Singh, M.K., Maiti, D., Manna, K., 2018. Role of plant alkaloids on human health: a review of biological activities. Mater. Today Chem. 9, 56–72.

El-Hawary, S.S., Moawad, A.S., Bahr, H.S., Ramadanabdelmohsen, U., Mohammed, R., 2020. Natural product diversity from the endophytic fungi of the genus *Aspergillus*. RSC Adv. 10, 22058–22079.

Hagag, A., Abdelwahab, M.F., El-Kader, A., Fouad, M.A., 2022. The endophytic *Aspergillus* strains: a bountiful source of natural products. J. Appl. Microbiol. 132 (6), 4150–4169.

Hu, Q.F., Liao, L.M., Huang, H.T., Xu, Y., Wang, J., Kong, W.S., Mi, Q.L., Zhou, M., Yang, G.Y., Song, C.M., 2020. Two new isoquinoline alkaloids from whole plants of *Thalictrum glandulosissimum* and their anti-TMV activity. Chem. Nat. Compd. 56, 500–503.

Hu, Q.F., Ma, Y.Y., Liu, H.Y., Dai, J.M., Yang, F.X., Zhang, J.D., Wang, J., Li, X.M., Liu, X., Li, J., Li, Y.K., Wang, W.G., Zhou, M., Yang, G.Y., 2022. Antivirus isoindolinone alkaloids with rare oxocyclopenta*[ff]*isoindole frameworks isolated from the stems of flue cured tobacco. Chem. Biol. Technol. Agric. 9, 88.

Kohno, J., Hiramatsu, H., Nishio, M., Sakurai, M., Okuda, T., Komatsubara, S., 1999. Structures of TMC-120A, B and C, novel isoquinoline alkaloids from *Aspergillus ustus* TC 1118. Tetrahedron 55, 11247–11252.

Li, Q., Chen, C.M., He, Y., Wei, M.S., Cheng, L., Kang, X., Wang, J.P., Hao, X.C., Zhu, H. C., Zhang, Y.H., 2020a. Prenylated quinolinone alkaloids and prenylated isoindolinone alkaloids from the fungus *Aspergillus nidulans*. Phytochemistry 169, 112–177.

Li, J.J., Zhao, Y.Y., Qin, Y.Q., Shi, H.Z., 2020b. Influence of microbiota and metabolites on the quality of tobacco during fermentation. BMC Microbiol 20, 356.

Liu, C.M., Yao, F.H., Lu, X.H., Zhang, X.X., Luo, L.X., Liang, X., Qi, S.H., 2022. Isoquinoline alkaloids as protein tyrosine phosphatase inhibitors from a deep-sea-derived fungus *Aspergillus puniceus*. Mar. Drugs 20, 78.

Luo, D., Lv, N., Zhu, L.J., Liao, L.M., Xu, Y., Wang, J., Kong, W.S., Huang, H.T., Zhou, M., Yang, G.Y., Hu, Q.F., Si, X.X., 2020. Isoquinoline alkaloids from whole plants of *Thalictrum cirrhosum* and their antirotavirus activity. Chem. Nat. Compd. 56, 504–508.

Moradi, M.T., Karimi, A., Lorigooini, Z., 2018. Alkaloids as the natural anti-influenza virus agents: a systematic review. Toxin Rev. 37, 11–18.

Nord, C., Levenfors, J.J., Bjerketorp, J., Sahlberg, C., Guss, B., Ober, B., Broberg, A., 2019. Antibacterial isoquinoline alkaloids from the fungus *Penicillium spathulatum* Em19. Molecules 24 (4616).

Prabal, G., Gopinatha, S.K., 2010. Isoquinoline alkaloids and their binding with polyadenylic acid: potential basis of therapeutic action. Mini-Rev. Med. Chem. 10, 568–577.

Qing, Z.X., Yang, P., Tang, Q., Cheng, P., Liu, X.B., Zheng, Y.J., Liu, Y.S., Zeng, J.G., 2017. Isoquinoline alkaloids and their antiviral, antibacterial, and antifungal activities and structure-activity relationship. Curr. Org. Chem. 21, 1920-1 34.

Quang, D.N., Schmidt, J., Porzel, A., Wessjohann, L., Haid, M., Arnold, N., 2010. Ampullosine, a new Isoquinoline Alkaloid from *Sepedonium ampullosporum* (Ascomycetes). Nat. Prod. Commun. 5, 869–872.

Sun, H.W., Zhang, K., Long, J., Zhang, X.W., Zhang, J.W., Cai, J.Y., Ma, X.W., Feng, X., Shu, Y.B., Wei, J., Liu, Y.C., 2020. Study on the appearance quality evaluation of cigar leaf in Yunnan Province. Chin. J. Mod. Agr. Sci. Tech. 14, 211–214.

Toghueo, R., Sahal, D., Boyom, F.F., 2020. Recent advances in inducing endophytic fungal specialized metabolites using small molecule elicitors including epigenetic modifiers. Phytochemistry 174, 112338.

Wang, W.G., Du, L.Q., Sheng, S.L., Li, A., Li, Y.P., Cheng, G.G., Li, G.P., Sun, G.L., Hu, Q. F., Matsuda, Y., 2019. Genome mining for fungal polyketide-diterpenoid hybrids: discovery of key terpene cyclases and multifunctional P450s for structural diversification. Org. Chem. Front. 6, 571–578.

Yadav, P., Shah, K., 2021. Quinolines, a perpetual, multipurpose scaffold in medicinal chemistry. Bioorg. Chem. 109, 104639.

Yang, F.X., Dai, J.M., Liu, H.Y., Mi, Q.L., Wang, J., Zhang, J.D., Li, X.M., Wang, W.G., Zhou, M., Li, Y.K., Hu, Q.F., 2022a. Isochromenes from the *Nicotiana tabacum*-derived endophytic fungus *Aspergillus versicolor* and their anti-tobacco mosaic virus activities. Nat. Prod. Res. 36 (published on-line).

Yang, G.Y., Dai, J.M., Mi, Q.L., Li, Z.J., Li, X.M., Zhang, J.D., Wang, J., Li, Y.K., Wang, W. G., Zhou, M., Hu, Q.F., 2022b. Cyclopiazonic acid type indole alkaloids from *Nicotiana tabacum*-derived fungus *Aspergillus versicolor* and their anti-tobacco mosaic virus activities. Phytochemistry 198, 113137.

Yang, G.Y., Dai, J.M., Li, Z.J., Wang, J., Yang, F.X., Liu, X., Li, J., Gao, Q., Li, X.M., Li, Y. K., Wang, W.G., Zhou, M., Hu, Q.F., 2022c. Isoindolin-1-ones from the stems of *Nicotiana tabacum* and their antiviral activities. Arch. Pharm. Res. 45, 572–583.

Yin, Gun, Zhu, Y.N., Wu, F., Mi, Q.L., Shi, J.Q., Gao, Q., Zhu, L.C., Zhou, T., Li, J., Liu, X., Yang, G.Y., Hu, Q.F., Kong, W.S., 2022. Two new antibacterial chromeno[3,2-*c*] pyridine alkaloids from whole plants of *Thalictrum scabrifolium*. Chem. Nat. Compd. 58, 506–510.

Zheng, L.L., Zhao, L., Cai, X.H., Chen, Z., Chai, Z.S., Shi, X.D., 2022. Analysis of bacterial and fungal community diversity during industrial secondary fermentation of cigar core tobacco leaves. Acta Tab. Sin. 28, 121–128.

Zheng, R.H., Li, S.J., Zhang, X., Zhao, C.Q., 2021. Biological activities of some new secondary metabolites isolated from endophytic fungi: a review study. Int. J. Mol. Sci. 22, 959.

Zhou, M., Lou, J., Li, Y.K., Wang, Y.D., Zhou, K., Ji, B.K., Dong, W., Gao, X.M., Du, G., Hu, Q.F., 2015a. Butyrolactones from the endophytic fungus *Aspergillus versicolor* and their Anti-Tobacco Mosaic Virus. Act. J. Braz. Chem. Soc. 26, 545–549.

Zhou, M., Du, G., Yang, H.Y., Xia, C.F., Yang, J.X., Ye, Y.Q., Gao, X.M., Li, X.N., Hu, Q.F., 2015b. Antiviral butyrolactones from the endophytic fungus *Aspergillus versicolor*. Planta Med. 81, 235–240.

Zhou, M., Zhou, K., He, P., Wang, K.M., Zhu, R.Z., Wang, Y.D., Dong, W., Li, G.P., Yang, H.Y., Ye, Y.Q., Du, G., Li, X.M., Hu, Q.F., 2016. Antiviral and cytotoxic isocoumarin derivatives from an endophytic fungus *Aspergillus oryzae*. Planta Med. 82, 414–417.